

# A systematic study on the crystal structure and properties of $\text{RuSr}_2\text{RCu}_2\text{O}_{8-\delta}$ ( $R = \text{Gd, Tb, Dy, Y, Ho, Er}$ )

L.T. Yang,<sup>a,\*</sup> J.K. Liang,<sup>a,b,1</sup> Q.L. Liu,<sup>a</sup> C.Q. Jin,<sup>a</sup> X.M. Feng,<sup>a</sup> G.B. Song,<sup>a</sup> J. Luo,<sup>a</sup> F.S. Liu,<sup>a</sup> and G.H. Rao<sup>a</sup>

<sup>a</sup>*Institute of Physics and Center for Condensed Matter Physics, Laboratory of Optical Physics, Chinese Academy of Sciences, P.O. Box 603, Beijing 100080, PR China*

<sup>b</sup>*International Center for Materials Physics, Academia Sinica, Shenyang 110016, PR China*

Received 13 July 2003; received in revised form 4 October 2003; accepted 14 October 2003

## Abstract

The coexistence of superconductivity and magnetic order seems to take place in the so-called ruthenate-cuprates (Ru-1212). A systematic study is carried out on crystal structure of the  $\text{RuSr}_2\text{RCu}_2\text{O}_{8-\delta}$  phases ( $R = \text{Gd, Tb, Dy, Y, Ho, Er}$ ) synthesized under high pressure by X-ray powder diffraction.  $\text{RuSr}_2\text{RCu}_2\text{O}_{8-\delta}$  ( $R = \text{Gd, Tb, Dy, Y, Ho, Er}$ ) has the Ru-1212-type structure of a tetragonal symmetry and the  $\text{RuO}_6$  octahedra rotate around the  $c$ -axis with an additional small rotation around an axis perpendicular to  $c$ . The DC-magnetization data establish that compounds with  $R = \text{Gd, Y, Ho, Er}$  exhibit ferromagnetic order below about 140 K, and the Meissner effect was observed at low temperature for  $R = \text{Y}$  compound.

© 2003 Elsevier Inc. All rights reserved.

**Keywords:** Ru-1212; Crystal structure; High-pressure synthesis; X-ray diffraction

## 1. Introduction

The crystal structure, i.e., the arrangement of atoms in a material, largely determines its physical properties. Precise structure determination is one of the basic requirements for any new substance. This is particularly true for the high- $T_c$  perovskite-type compounds whose superconducting properties are strongly related to the structural details.

Recent discovery of the coexistence of superconductivity (SC) and ferromagnetism (FM) in the ruthenate-cuprate compounds  $\text{RuSr}_2\text{RCu}_2\text{O}_{8-\delta}$  with  $R = \text{Sm, Gd, Eu}$  [1–8] has raised widespread interest in these compounds. The ferromagnetic (FM)-like order appears at a rather higher Curie temperature of  $T_M = 130$ – $150$  K, whereas SC occurs at a significantly lower superconducting (SC) transition temperature  $T_c = 15$ – $45$  K [6]. They have thus been called as FM superconductors.

From neutron scattering it is established that the Ru ions display predominantly a G-type antiferromagnetic structure [7]. The ferromagnetic moment which has been observed in magnetization measurements results from the rotation of the  $\text{RuO}_6$  octahedra about an axis perpendicular to  $c$ , leading to finite antisymmetric exchange interactions and probably a slight canting of the Ru moments. From the neutron diffraction an upper limit of  $0.1 \mu_B$  was derived for the ferromagnetic moment [7].

In the Ru-1212 family  $\text{RuSr}_2\text{RCu}_2\text{O}_{8-\delta}$ , rare-earth element with larger ionic radius, such as Sm, Eu and Gd can occupy the  $R$  site, but rare-earth elements with ionic radius smaller than that of Gd can not form Ru-1212 phase under ambient pressure. It is expected that under high pressure smaller rare-earth ions may accommodate themselves to the  $\text{RO}_8$  site of Ru-1212 because under this condition the contraction of oxygen ions (anions) could be larger than that of rare-earth ions (cations). Indeed, we successfully prepared single phase compounds  $\text{RuSr}_2\text{RCu}_2\text{O}_{8-\delta}$  ( $R = \text{Tb, Dy, Y, Ho, Er}$ ) at 5.5 GPa by using precursory materials  $\text{Sr}_2\text{RRuO}_6$  (Sr-2116) and CuO. The crystal structure of the  $\text{RuSr}_2\text{RCu}_2\text{O}_{8-\delta}$  ( $R = \text{Tb, Dy, Y, Ho, Er}$ ) synthesized

\*Corresponding author. Fax: +86-01-826495631.

E-mail addresses: [lyang@aphy.iphy.ac.cn](mailto:lyang@aphy.iphy.ac.cn) (L.T. Yang), [jkliang@aphy.iphy.ac.cn](mailto:jkliang@aphy.iphy.ac.cn) (J.K. Liang).

<sup>1</sup>Also for correspondence

under high pressure were carefully characterized using X-ray powder diffraction (XRD). In order to clarify the magnetic and electrical properties of  $\text{RuSr}_2\text{RCu}_2\text{O}_{8-\delta}$  ( $R = \text{Tb, Dy, Y, Ho, Er}$ ) compound, magnetic and electric measurements were also performed for  $R = \text{Y, Ho, Er}$  in this paper.

## 2. Experiment

Compounds  $\text{RuSr}_2\text{RCu}_2\text{O}_{8-\delta}$  ( $R = \text{Tb, Dy, Y, Ho, Er, Tm, Yb}$ ) were synthesized by using precursor material  $\text{Sr}_2\text{RRuO}_6$  and  $\text{CuO}$ . The  $\text{Sr}_2\text{RRuO}_6$  materials were prepared by solid-state reactions in the air. Starting materials high purity ( $>99.9\%$ )  $\text{SrCO}_3$ ,  $\text{RuO}_2$ ,  $\text{Eu}_2\text{O}_3$ ,  $\text{Gd}_2\text{O}_3$ ,  $\text{Tb}_2\text{O}_3$ ,  $\text{Dy}_2\text{O}_3$ ,  $\text{Y}_2\text{O}_3$ ,  $\text{Ho}_2\text{O}_3$ ,  $\text{Er}_2\text{O}_3$ ,  $\text{Tm}_2\text{O}_3$  and  $\text{Yb}_2\text{O}_3$  were used. The raw powder was preheated separately at  $200^\circ\text{C}$  for 5 h and weighted according to the stoichiometric compositions, calcined at  $900^\circ\text{C}$  for 12 h in air in order to achieve decomposition of the carbonates, then ground and pressed into pellets, and heated at  $1250^\circ\text{C}$  in an oxygen atmosphere for 24 h. The precursory  $\text{Sr}_2\text{RRuO}_6$  and  $\text{CuO}$  powders were weighed in the stoichiometric ratio and mixed. The mixture in a sealed gold cell was sintered in a high-pressure furnace at  $1100\text{--}1200^\circ\text{C}$  for 0.5 h under a pressure of about 5.5 GPa. For the convenience of discussing the structure data for this system, we also synthesized the compound for  $R = \text{Gd}$  under normal pressure.

XRD data used for structural analyses were collected on a Rigaku D/max 2500 diffractometer with  $\text{CuK}\alpha$  radiation ( $40\text{ kV} \times 250\text{ mA}$ ) and a graphite monochromator. A step scan mode was employed with a step width of  $2\theta = 0.02^\circ$  and a sampling time of 1 s. The XRD data were analyzed by the Rietveld refinement program DBWS-9411 [9,10]. XRD patterns show that samples with  $R = \text{Tb, Dy, Y, Ho, Er}$  are single phase with the tetragonal Ru-1212 structure, but samples with  $R = \text{Tm}$  and  $\text{Yb}$  contains two phases ( $\text{Sr}_2\text{RRuO}_6$  and  $\text{CuO}$ ), as their ionic radius maybe is too small.

Temperature dependence of magnetization was measured by a superconducting quantum interference device (SQUID) magnetometer. Electrical resistance was measured by the standard four-probe method from 300 down to 5 K in the zero field.

## 3. Results and discussion

### 3.1. Structure refinement

For the structure of  $\text{RuSr}_2\text{GdCu}_2\text{O}_{8-\delta}$  compound the  $\text{RuO}_6$  polyhedron is almost an ideal octahedron [6,11]. Synchrotron X-ray diffraction experiment suggested an existence of small deviation of apical oxygen ions in the  $\text{RuO}_6$  octahedron from  $(00z)$  position along a plane

perpendicular to the  $c$ -axis [2], which could explain the origin of the ferromagnetic moment observed in magnetization measurements. In our work, a small  $R_{\text{wp}}$  factors were achieved for the refinement with the apical oxygen displaced from the  $(00z)$  to the  $(x0z)$  position.

The XRD data of the compounds  $\text{RuSr}_2\text{RCu}_2\text{O}_{8-\delta}$  ( $R = \text{Gd, Tb, Dy, Y, Ho, Er}$ ) for the  $2\theta$  region between  $20^\circ$  and  $80^\circ$  were used for the refinement of the structure. The XRD patterns (Fig. 1) show that all samples are single phase and could be completely indexed on the basis of the tetragonal space group  $P4/mmm$  in which Ru ions occupy the crystallographic  $1b$  site  $(0, 0, 1/2)$ , rare-earth ions the  $1c$  site  $(1/2, 1/2, 0)$ , Sr ions the  $2h$  site  $(1/2, 1/2, z)$ , Cu the  $2g$  position  $(0, 0, z)$ , and  $2\text{O}(1)$  in  $8s$  position  $(x, 0, z)$  with a occupancy of  $1/4$ ,  $4\text{O}(2)$  in  $4i$   $(0, 1/2, z)$ , and  $2\text{O}(3)$  in  $4o$  position  $(x, 1/2, 1/2)$  with an occupancy of  $1/2$ , respectively. Fig. 2 shows the structural model of  $\text{RuSr}_2\text{RCu}_2\text{O}_8$ . The crystallographic structure is closely related to that of other 1212-type cuprate superconductors. The  $\text{RuO}_6$  octahedra are connected via their apical oxygen ion with  $\text{CuO}_5$  square single pyramids. The bond angle of  $\text{Ru-O}(1)\text{-Cu}$  ions, which is characteristic for distortions of the  $\text{RuO}_6$  octahedra, is essential for the magnetic exchange interaction and the charge transfer between the  $\text{Ru-O}$  and  $\text{Cu-O}$  layer.

Table 1 shows final results of the Rietveld refinements for the  $\text{RuSr}_2\text{RCu}_2\text{O}_{8-\delta}$  ( $R = \text{Gd, Tb, Dy, Y, Ho, Er}$ ) compounds in space group  $P4/mmm$ . Typical fitting results for  $\text{RuSr}_2\text{RCu}_2\text{O}_{8-\delta}$  ( $R = \text{Dy}$  and  $\text{Ho}$ ) are shown in Figs. 3(a) and (b), respectively. The spots and solid curves are the observed and the calculated intensities, respectively. The vertical bars at the top indicate the expected Bragg reflection positions, and the curve in the bottom is the difference between the observed and the calculated patterns.

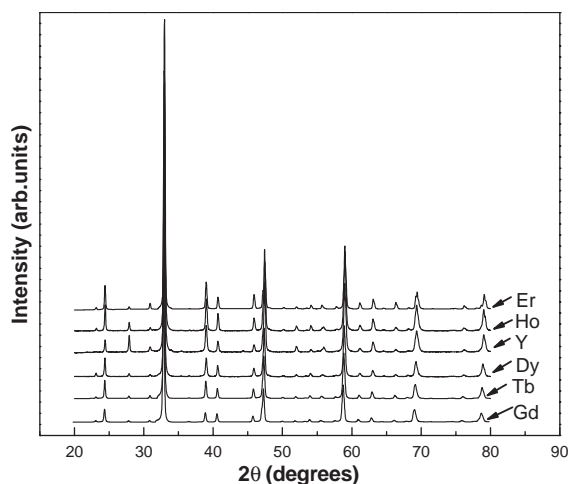


Fig. 1. XRD patterns of  $\text{RuSr}_2\text{RCu}_2\text{O}_{8-\delta}$  ( $R = \text{Gd, Tb, Dy, Y, Ho}$  and  $\text{Er}$ ).

Fig. 4 show the lattice parameters  $a$ ,  $c/3$  and the unit cell volume of the compounds  $\text{RuSr}_2\text{RCu}_2\text{O}_{8-\delta}$  ( $R = \text{Gd, Tb, Dy, Y, Ho, Er}$ ) versus radius of trivalent  $R$  ions ( $\text{CN} = 8$ ). Fig. 4 clearly shows the expected lanthanide contraction behavior, i.e., and a perfectly linear relationship of the lattice parameters versus the ionic radius of trivalent rare-earth ions.

Table 2 lists the selected interatomic distances and coordination numbers of the tetragonal  $\text{RuSr}_2\text{RCu}_2\text{O}_{8-\delta}$  compounds. To examine the reliability of the determined structure, we used the bond valence model to estimate the valence of the ions. The valences of the

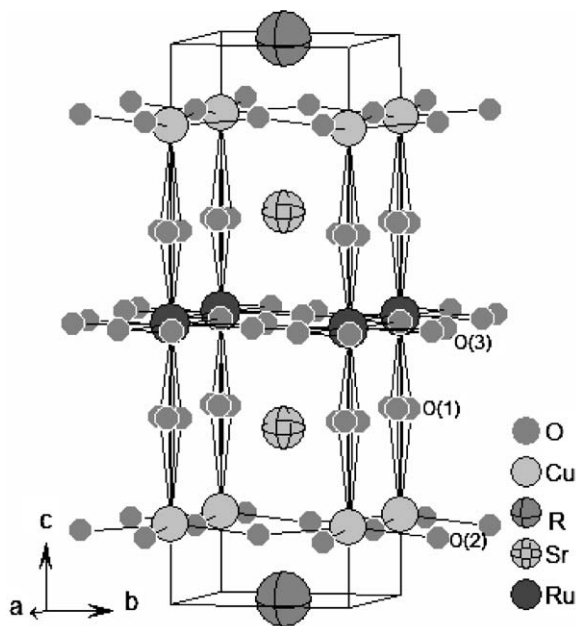


Fig. 2. Illustration of the crystal structure of  $\text{RuSr}_2\text{RCu}_2\text{O}_{8-\delta}$ .

$\text{Sr}$ ,  $R$ ,  $\text{Ru}$  and  $\text{Cu}$  atom are estimated as shown in Table 3 with a Zachariasen–Brown–Altermatt formula [12]. The value of  $r_0$  for  $\text{Ru}^{5+}$  is  $1.9025 \text{ \AA}$  which is calculated by the equation derived from Ref [12]. The

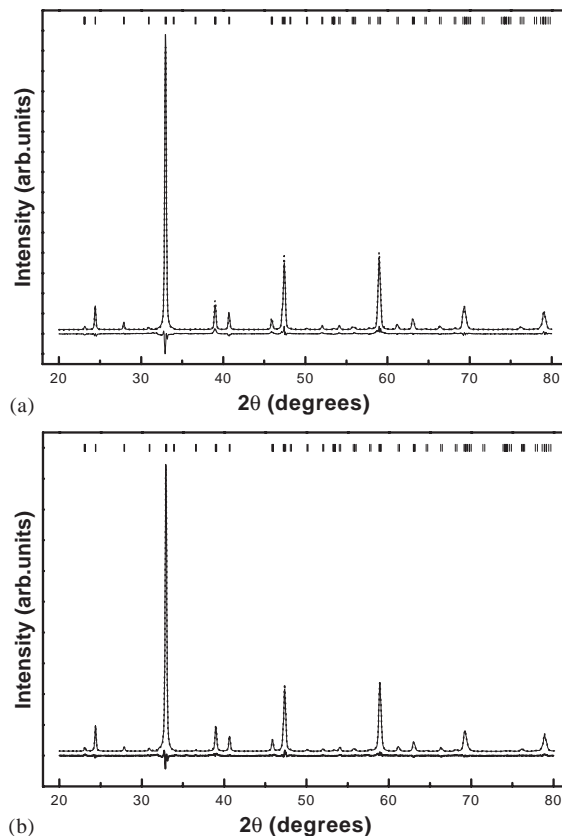


Fig. 3. Observed, calculated and difference XRD patterns of: (a)  $\text{RuSr}_2\text{DyCu}_2\text{O}_{8-\delta}$ ; (b)  $\text{RuSr}_2\text{HoCu}_2\text{O}_{8-\delta}$  at 300 K. The vertical bars at the top indicate Bragg reflection positions.

Table 1

Final results of the Rietveld refinements for the  $\text{RuSr}_2\text{RCu}_2\text{O}_{8-\delta}$  ( $R = \text{Gd, Tb, Dy, Y, Ho}$  and  $\text{Er}$ )

$R$	Gd	Tb	Dy	Y	Ho	Er
Radius for $R^{3+}$ ( $\text{\AA}$ )	1.053	1.04	1.027	1.019	1.015	1.004
$R_{\text{wp}}$	5.89%	4.63%	3.43%	3.91%	4.60%	4.86%
$R_{\text{p}}$	8.99%	6.63%	4.62%	5.50%	6.37%	6.82%
$R_{\text{exp}}$	2.48%	1.93%	1.99%	1.58%	1.78%	1.80%
$a$ ( $\text{\AA}$ )	3.8410(1)	3.8368(1)	3.8309(2)	3.8275(1)	3.8260(3)	3.8209(1)
$c/3$ ( $\text{\AA}$ )	3.8577(1)	3.8515(3)	3.8468(1)	3.8442(1)	3.8433(1)	3.8385(4)
$V$ ( $\text{\AA}^3$ )	170.741	170.093	169.365	168.949	168.778	168.118
$Z_{\text{Sr}}$	0.3071(2)	0.3076(3)	0.3071(5)	0.3068(5)	0.3076(1)	0.3081(5)
$Z_{\text{Cu}}$	0.1454(3)	0.1453(4)	0.1448(3)	0.1446(2)	0.1423(7)	0.1421(5)
$X_{\text{O}(1)}$	0.0602(8)	0.0395(11)	0.0493(7)	0.0313(3)	0.0375(12)	0.0612(4)
$Z_{\text{O}(1)}$	0.3342(12)	0.3332(8)	0.3335(11)	0.3325(8)	0.3328(4)	0.3331(7)
$Z_{\text{O}(2)}$	0.1294(8)	0.1245(7)	0.1215(6)	0.1234(13)	0.1244(7)	0.1211(3)
$X_{\text{O}(3)}$	0.1446(4)	0.1485(11)	0.1503(6)	0.14999(6)	0.1518(8)	0.1501(10)
$\text{Occ}_{\text{O}(3)}$	0.49	0.43	0.46	0.44	0.42	0.46
$\phi$ (deg)	167.09	171.51	169.43	173.29	172.01	166.99

Note: The occupancy factors for O(1) and O(2) were kept fixed at the value 0.25 and 1. The temperature factors for all the atoms were also kept fixed at the value 0.5 in our refinement.

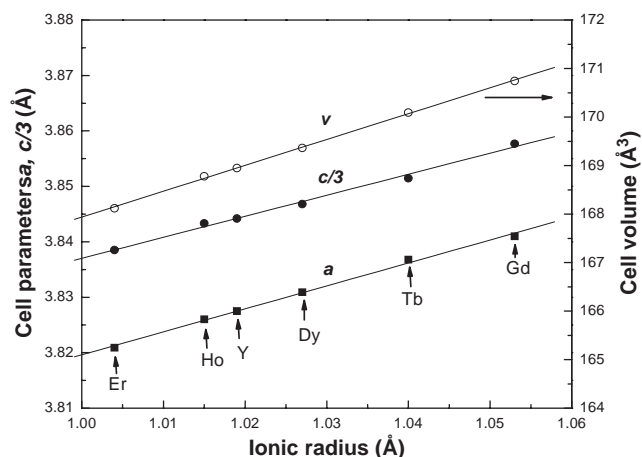


Fig. 4. Lattice parameters  $a$ ,  $c/3$  and cell volume of  $\text{RuSr}_2\text{RCu}_2\text{O}_{8-\delta}$  ( $R = \text{Gd, Tb, Dy, Y, Ho}$  and  $\text{Er}$ ) versus radius of trivalent  $R$  ions.

Table 2

Selected bond distances ( $\text{\AA}$ ) and number of equivalent bonds,  $N$ , in the compounds  $\text{RuSr}_2\text{RCu}_2\text{O}_{8-\delta}$  ( $R = \text{Gd, Tb, Dy, Y, Ho, Er}$ )

$R$	Gd	Tb	Dy	Y	Ho	Er	$N$
Sr–O(1)	2.577	2.625	2.597	2.640	2.622	2.558	2
Sr–O(1)	2.901	2.838	2.862	2.808	2.824	2.886	2
Sr–O(2)	2.814	2.856	2.873	2.852	2.850	2.879	4
Sr–O(3)	2.615	2.598	2.598	2.600	2.590	2.583	2
Ln–O(2)	2.435	2.398	2.374	2.385	2.391	2.365	8
Ru–O(1)	1.933	1.933	1.931	1.935	1.933	1.936	2
Ru–O(3)	2.000	2.002	2.000	1.998	1.998	1.995	4
Cu–O(1)	2.197	2.176	2.186	2.170	2.201	2.212	1
Cu–O(2)	1.929	1.933	1.934	1.929	1.924	1.926	4

Table 3

Bond valence sums of the Sr,  $R$ , Ru and Cu

	Gd	Tb	Dy	Y	Ho	Er
$V_{\text{Sr}}$	1.948	1.884	1.682	1.894	1.918	1.940
$V_{\text{Ln}}$	2.992	2.976	2.920	2.976	2.976	2.888
$V_{\text{Ru}}$	4.913	4.894	4.926	4.922	4.934	4.941
$V_{\text{Cu}}$	2.283	2.270	2.26	2.31	2.308	2.289

Note: The value of  $r_0$  for  $\text{Ru}^{5+}$  is  $1.9025 \text{\AA}$  which is calculated by the equation reported in Ref. [12].

results shown in Table 3 indicated that the valence of Ru ions is nearly 5 in Ru-1212 system. One can also see that the bond valences of Sr,  $R$  and Cu are close to their chemical valences of the ions. These suggest that the structure determined by the Rietveld refinement is reliable.

### 3.2. Magnetization and electrical resistance

The magnetic moment derived from magnetization measurements for the Gd compound must be due to the

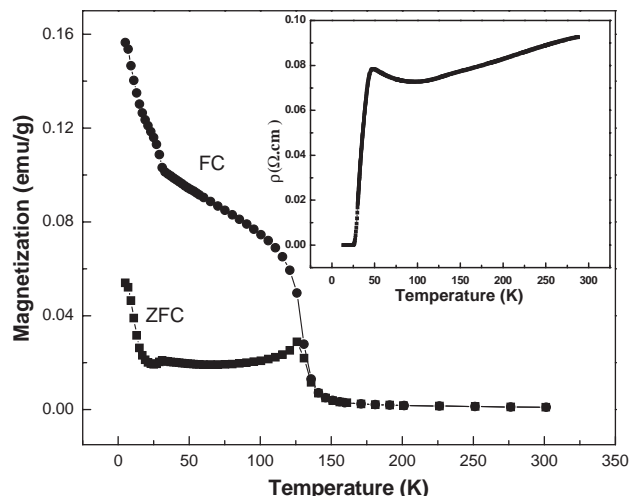


Fig. 5. Temperature ( $T$ ) dependence of magnetization ( $M$ ) of  $\text{RuSr}_2\text{GdCu}_2\text{O}_{8-\delta}$  measured at 20 Oe. The upper inset shows the temperature dependence of the resistivity under zero field.

rotation of the  $\text{RuO}_6$  octahedra about an axis perpendicular to  $c$ , resulting in finite antisymmetric exchange interactions and probably a slight canting of the Ru moments. The temperature dependence of magnetization and resistivity for  $\text{RuSr}_2\text{GdCu}_2\text{O}_{8-\delta}$  shown in Fig. 5 and its insert indicate that ferromagnetic transition temperature  $T_M$  and zero resistivity temperature ( $T_c^2$ ) are 131 and 16 K, respectively. The zero resistivity temperature coincides with previous report [6]. The ZFC and FC curves show a large magnetization increase at low temperature, which results from the paramagnetic contribution of Gd ion [13]. No Meissner effect is observed below  $T_c$  (see Fig. 5) for this sample as the small negative magnetization resulting from intragranular supercurrents is swamped by the positive contributions from Ru and paramagnetic Gd moments [14].

Fig 6a shows the field-cooled and zero-field-cooled temperature dependence of the magnetization ( $M$ ) of  $\text{RuSr}_2\text{YCu}_2\text{O}_{8-\delta}$  in an external magnetic field 100 Oe. The magnetic transition can be seen at about  $T_M = 145 \text{ K}$ , where  $dM/dT$  exhibits a minimum. The behavior is similar to that of Ru-1212 ( $R = \text{Gd}$ ). The insert of Fig. 6a shows the temperature dependence of the resistivity under zero field. One can see that the onset of superconducting transition temperature is about 45 K and resistivity becomes to zero at about 28 K, this result is consistent with it reported in literature [15]. Differing from the Gd sample, the zero-field-cooled curve of Y compound exhibits the Meissner effect in the low temperature part. This difference may attribute to the decrease of the contribution of the rare-earth atom sites since Y is non-magnetic. Takagiwa et al. [15] reported no Meissner effect for the Y-compound, which may be due to the sample preparation conditions.

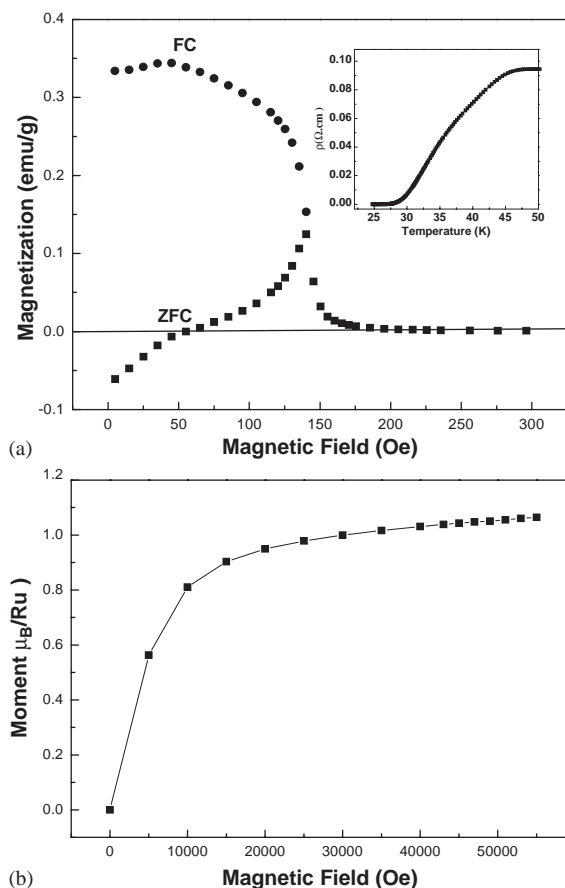


Fig. 6. (a) ZFC and FC magnetization curves for  $\text{RuSr}_2\text{YCu}_2\text{O}_{8-\delta}$  measured at 100 Oe. The insert shows the temperature dependence of the resistivity under zero field. (b) The magnetic field dependence of the magnetization at 5 K.

Fig. 6b shows the magnetic field dependence of the magnetization at 5 K. The magnetization curve is strongly dependent on the magnetic field up to about  $H = 3$  T. The magnetization is likely to approach saturating at  $H = 5.5$  T and the saturation magnetic moment is  $\mu_s = 1.17 \mu_B$ . This value corresponds to the magnetic component of the Ru sublattice since the rare-earth Y is non-magnetic ion. The number of  $4d$  electrons for  $\text{Ru}^{5+}$  is 3 and therefore the magnetic moment of the free-ion is  $3 \mu_B$  for the high-spin state and  $1 \mu_B$  for the low-spin state.

The ZFC temperature dependence of magnetization measured at 100 Oe for  $\text{RuSr}_2\text{HoCu}_2\text{O}_{8-\delta}$  is shown in Fig. 7a. The insert shows the temperature dependence of the resistivity under zero field from 5 to 300 K. Same as the Gd and Y compound, one can see  $\text{RuSr}_2\text{HoCu}_2\text{O}_{8-\delta}$  exhibits a ferromagnetic to paramagnetic transition at the  $T_M = 136$  K. A metal-insulator transition can be clearly seen at about 22 K from the electrical resistance data. We cannot confirm it was a superconducting transition due to the resistivity does not reach zero until 4.2 K.  $M(H)$  curves of  $\text{RuSr}_2\text{HoCu}_2\text{O}_{8-\delta}$  is presented in

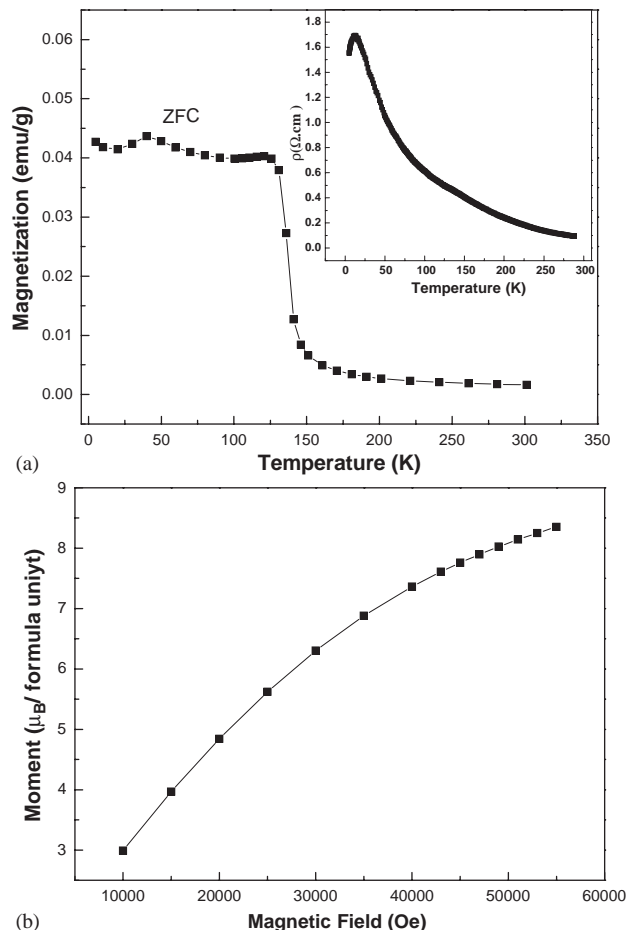


Fig. 7. (a) ZFC magnetization curve for  $\text{RuSr}_2\text{HoCu}_2\text{O}_{8-\delta}$  measured at 100 Oe, and the insert shows the temperature dependence of the resistivity under zero field. (b) The magnetic field dependence of the magnetization at 5 K.

Fig. 7b. At 5 K, the magnetization does not show saturation until 5.5 kOe. We estimate the saturation magnetic moment  $\mu_s = 9.50 \mu_B$  by extrapolation. This value is lower than  $10.60 \mu_B$ , the theoretical saturation moment of  $\text{Ho}^{3+}$  ion. On the other hand, the experimentally observed value of  $\mu(\text{Ru}) = 1.17 \mu_B$  obtained from our Y compound. This may indicate that magnetic moments of Ho and Ru are antiparallel to each other.

Fig. 8a shows the temperature dependence of the magnetization measured at 100 Oe for  $\text{RuSr}_2\text{ErCu}_2\text{O}_{8-\delta}$ . The ferromagnetic transition takes place at about 143 K. The low-temperature magnetization (Fig. 8b) can approach almost to saturating at a value  $\mu_{\text{sat}} = 6.75 \mu_B$ , which is very close to the difference between the theoretical moment of  $\text{Er}^{3+}$  ( $8 \mu_B$ ) and the Ru moment ( $1.17 \mu_B$ ). Electric resistivity measurement shows that  $R = \text{Er}$  compound exhibits a semiconductor behavior down to the 4.2 K (see the insert Fig. 8a). Compounds with  $R = \text{Tb}$  and  $\text{Dy}$  also exhibit non-superconducting behavior down to 4.2 K based on electric resistivity measurement (not shown here).



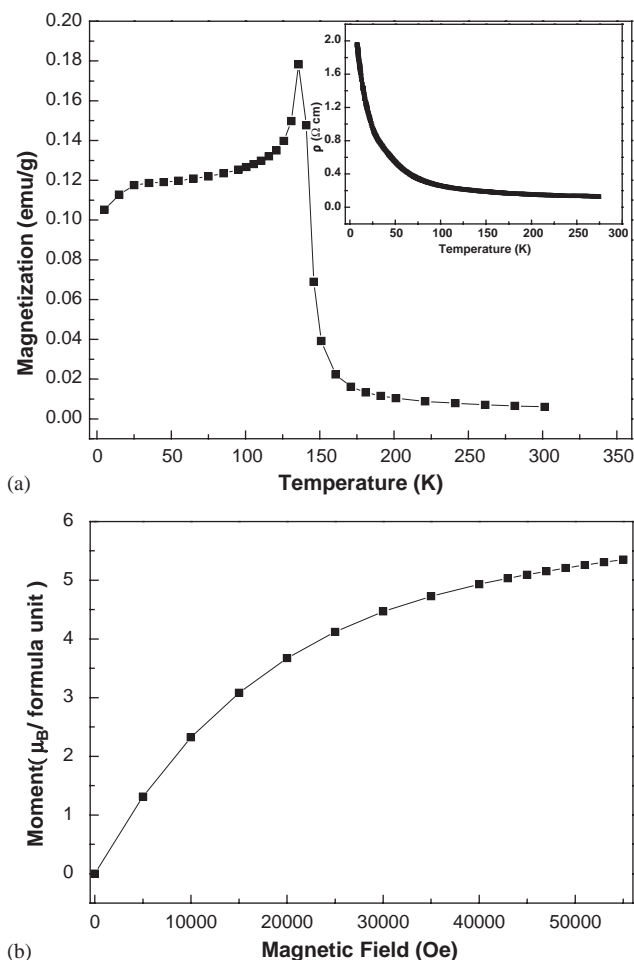


Fig. 8. (a) ZFC magnetization curve for RuSr<sub>2</sub>ErCu<sub>2</sub>O<sub>8-δ</sub> measured at 100 Oe, and the insert shows the temperature dependence of the resistivity under zero field. (b) The magnetic field dependence of the magnetization at 5 K.

Compounds RuSr<sub>2</sub>RCu<sub>2</sub>O<sub>8-δ</sub> ( $R = Y, Ho, Er$ ) exhibit magnetic transitions at the  $T_M$  about 140 K. The sharp increase in the susceptibility observed at around about 140 K can be attributed to the Dzialoshinsky–Moriya ferromagnetic component due to the spin canting in the  $a-b$  plane of the antiferromagnetically ordered Ruthenium moments along the  $c$ -axis, as recently reported by Lynn et al. in the case of the isostructural Gd rutheno-cuprate. Compounds RuSr<sub>2</sub>RCu<sub>2</sub>O<sub>8-δ</sub> with  $R = Sm, Eu,$  and Gd exhibited SC, while isostructural compounds with  $R = Tb, Dy, Ho,$  and Er show non-superconducting behavior down to 4.2 K. This result may reflect the difference of the electronic structure for lanthanide, as we known the number of  $4f$  electrons  $\leq 7$  for  $R = Sm, Eu,$  and Gd, which for  $R = Tb, Dy, Ho,$  and Er the number of  $4f$  electrons  $> 7$ .

#### 4. Conclusion

The crystal structure are systematically studied of the phases RuSr<sub>2</sub>RCu<sub>2</sub>O<sub>8-δ</sub> ( $R = Gd, Tb, Dy, Y, Ho, Er$ ) by Rietveld refinement method. They belong to a tetragonal system, and lattice parameters  $a, c/3$  and the unit cell volume clearly shows the expected lanthanide contraction. Magnetic measurements indicate that  $R = Y, Ho$  and Er compounds exhibit the same ferromagnetic transition behavior as Gd compound. The Y sample is superconducting and the  $T_c^z$  increases from about 16 K (in the Gd compound) to 30 K. A metallic to semiconductor transition was observed in low temperature region for Ho compound.

#### Acknowledgments

This work is supported by the State Key Project of Fundamental Research (NKBRF-G19990466) and by the National Natural Science Foundation of China (50272083). We thank J.R. Chen for the XRD and magnetic measurements.

#### References

- [1] L. Bauernfeind, W. Widder, H.F. Braun, Physica C 254 (1995) 151.
- [2] A.C. Mclaughlin, W. Zhou, J.P. Attfield, A.N. Fitch, J.L. Tallon, Phys. Rev. B 60 (1999) 7512.
- [3] J.L. Tallon, J.W. Loram, G.V.M. Williams, C. Bernhard, Phys. Rev. B 61 (2000) 6471.
- [4] C. Bernhard, J.L. Tallon, E. Brücher, R.K. Kremer, Phys. Rev. B 61 (2000) 14960.
- [5] C.W. Chu, Y.Y. Xue, S. Tsui, J. Cmaidalka, A.K. Heilman, B. Lorenz, R.L. Meng, Physica C 335 (2000) 231.
- [6] C. Bernhard, J.L. Tallon, Ch. Niedermayer, Th. Blasius, A. Golnik, E. Brücher, R.K. Kremer, D.R. Noakes, C.E. Stronach, E.J. Ansaldo, Phys. Rev. B 59 (1999) 14099.
- [7] J.W. Lynn, B. Keimer, C. Ulrich, C. Bernhard, J.L. Tallon, Phys. Rev. B 61 (2000) 14964.
- [8] G.V. Williams, S. Kramer, Phys. Rev. B 62 (2000) 4132.
- [9] H.M. Rietveld, Acta Crystallogr. 229 (1967) 151.
- [10] R.Y. Young, A. Sakthirel, T.S. Moss, C.O. Paiva-Santos, J. Appl. Crystallogr. 28 (1995) 336.
- [11] K.B. Tang, Y.T. Qian, L. Yang, Y.D. Zhao, Y.H. Zhang, Physica C 282 (1997) 947.
- [12] I.D. Brown, D. Altermatt, Acta Crystallogr. B 41 (1985) 244.
- [13] P. Mandal, A. Hassen, J. Hemberger, A. Krimmel, A. Loid, Phys. Rev. B 65 (2002) 144506.
- [14] A.C. Mclaughlin, J.P. Attfield, Phys. Rev. B 60 (1999) 14605.
- [15] Hiroyuki Takagiwa, Jun Akimitsu, Hazuki Kawano-Furukawa, Hideki Yoshizawa, J. Phys. Soc. Jpn. 70 (2001) 333.